Simulations of Large School Bus Safety Restraints - NHTSA

Linda McCray, National Highway Traffic Safety Administration
Aida Barsan-Anelli, Information Systems and Services, Inc.
Unites States of America
Paper Number 313

ABSTRACT

This paper describes computer crash simulations performed by the National Highway Traffic Safety Administration (NHTSA) under the current research and testing activities on large school bus safety restraints. The simulations of a frontal rigid barrier test and comparative dynamic sled testing for compartmentalization, lap belt, and lap/shoulder belt restraint strategies are presented.

School bus transportation is one of the safest forms of transportation in the United States. School age children transported in school buses are safer than children transported in motor vehicles of any other type. Large school buses provide protection because of their size and weight. Further, they must meet minimum Federal motor vehicle safety standards (FMVSSs) mandating compartmentalized seating, improved emergency exits, stronger roof structures and fuel systems, and better bus body joint strength.

INTRODUCTION

During the rulemaking process in the early 1970's, NHTSA looked carefully at available injury and fatality data, existing research, and public comments submitted to NHTSA to determine what system of occupant protection should be required in school buses when the school bus safety standards were established. Recognizing that school bus vehicles are heavier, experience lesser crash forces, and distribute crash forces differently than passenger cars and light trucks it was determined the best way to provide crash protection to children on large school buses was to use a concept called "compartmentalization." Compartmentalization is the method used to provide a protective envelope consisting of strong, well padded, well anchored, closely-spaced seats that have energy-absorbing seat backs. Compartmentalization, along with the enhanced safety standards such as joint integrity of the bus body panels and the stringent fuel system integrity requirements, make school buses the safest vehicles on the road.

Even though compartmentalization has proven to be an excellent concept for injury mitigation, NHTSA has initiated an extensive research program to develop the next generation occupant protection system(s).

NHTSA is currently conducting research to evaluate both currently available and prototype safety restraint systems in large school buses.

This paper will present the results and validation of computer simulations of a full-scale frontal rigid barrier crash test and two comparative dynamic sled tests. The simulations of compartmentalization, lap belt restraints and lap/shoulder belt restraints are presented to evaluate future occupant protection systems. Testing regarding the effects of seat back height and seat spacing on the performance of these safety restraint strategies are still under evaluation and, therefore, not included.

METHODS

A series of 13 sled tests were conducted to date to evaluate the performance of each restraint strategy. Three loading conditions were simulated: (1) belted occupants without any loading from occupants seated behind them, (2) belted occupants with loading from unbelted occupants seated behind them, and (3) unbelted occupants into the seat back in front of them. Two of the 13 sled tests, sled test #3 and sled test #6, were simulated. Sled test #3 contain loading condition (1) with lap belts and condition (3)for the 6 year old, 5th percentile adult female and 50th percentile adult male. Sled test #6 contain loading condition (1) with lap/shoulder belts for the 6 year old, 5th percentile adult female and 50th percentile adult male. The results of these tests, together with those of a frontal rigid barrier crash test are presented.

For each of the tests, the time histories of the school bus and sled tests were used to assess occupant kinematics. The MAthematical DYnamical MOdels program (MADYMO)[1] was used to simulate the

occupant kinematics for all three tests.

MADYMO is a general purpose software package that allows users to design and optimize occupant safety systems using both a rigid and flexible body.

MADYMO MODEL REPRESENTATION

Frontal Rigid Barrier Test

A frontal rigid barrier test was conducted by NHTSA at the Vehicle Research and Test Center (VRTC). A conventional style school bus (Class C) impacted a frontal rigid barrier at 30 mph. In order to evaluate safety enhancement devices for the whole range of sizes of people that school buses transport, NHTSA used the available Hybrid III anthropomorphic test devices (ATDs) -- the 6 year old, 5th percentile adult female and 50th percentile adult male. These dummies represent the average size 6-year-old child, 12-year-old adolescent, and large high school male, respectively. In the full-frontal crash test six Hybrid III ATDs were utilized – two 6 year olds, two 5th percentile adult females, and two 50th percentile adult males. Four uninstrumented Hybrid II ATDs were used as ballast; one 6 year old and three 50th percentile adult males. Figure 1 illustrates the occupant seating diagram. The instrumented ATDs are indicated.

Currently, NHTSA does not have seating procedures for positioning dummies in school bus sled and/or crash tests. The dummies were placed as upright and as far back in the seat as possible. Seat spacing was determined relative to the H-point location. Dummy position and seat measurements were taken and used for the simulations.

For the frontal rigid test, only three simulated occupants were considered for validation: occupant 1, occupant 3 and occupant 4. In the MADYMO modeling the Hybrid III 50th percentile adult male dummy was used for obtaining the occupant 1's kinematics, the Hybrid III 6 year old child dummy was used for occupant 3's kinematics, and the Hybrid III 5th percentile adult female dummy was used for obtaining the occupant 4's kinematics.

Default material properties, (from MADYMO User's Manual),[2] were used for the seats, windows and walls. The school bus seat was modeled in MADYMO using two ellipsoids, one for the seat cushion and one for the seat back. For most of the seats, the seat back was considered to be infinitely rigid. Due to severe impacts of some occupants into the seat in front of them, a considerably large deformation of the impacted seat was noticed in the actual crash test. For a more accurate simulation of the crash, this large plastic seat deformation was taken into account.

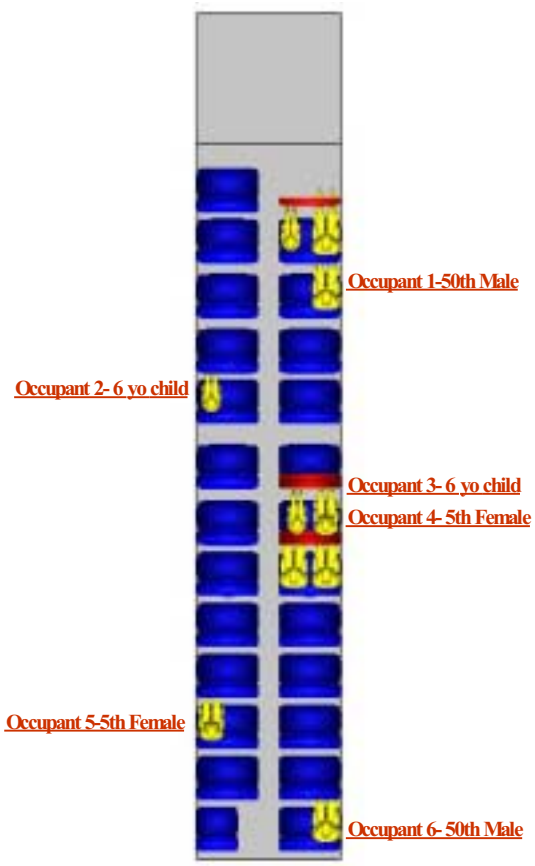

Figure 1. Occupant seating diagram for the full frontal rigid barrier test

Therefore, for those seats only, their backs were modeled so that they can rotate forward when severely impacted by the occupants. This was done in MADYMO by introducing a revolute joint between the two ellipsoids that were used to model the seat. The stiffness of the joint was defined using a certain torque-angle function. The following seats were modeled based on this assumption: the seat back of the seat located in front of occupant 1, the seat back of the seats in which occupants 3 and 4 were located, and the seat back in front of occupants 3 and 4. The school bus seat spacing ranged between 19 and 22 inches.

Sled Test #3

This simulation was performed on compartmentalized occupants and occupants in two-point belts. The rear seats of this test were standard

school bus seats with the lap belt option. The seats had a reinforced bench which accommodated the installation and loading forces of two-point belt restraint systems. The simulated occupant seating allowed analysis of the two -point restraint system for all available dummy sizes. There was no additional loading to the seat or seat back. The seat spacing was 19 inches. Figure 2 illustrates the passenger seating diagram and the seat belt representation as it appears in the MADYMO model.

Figure 2 illustrates the occupant seating diagram as it appears in the MADYMO model. All six occupants were modeled in MADYMO using the available Hybrid III 50th percentile adult male dummy, the Hybrid III 5th percentile adult female dummy and the Hybrid III 6 year old child dummy models in accordance with the dummies used in the actual sled test. Default material properties[3] were used for the seats. The same seat representation as in the full frontal rigid test MADYMO simulation described above was used to model large plastic deformations of the seat backs. The belts were constructed using membrane elements with the available finite elements in MADYMO. The belt attachment points were placed on the base of the seat pan and a certain slack function was defined for the belt.

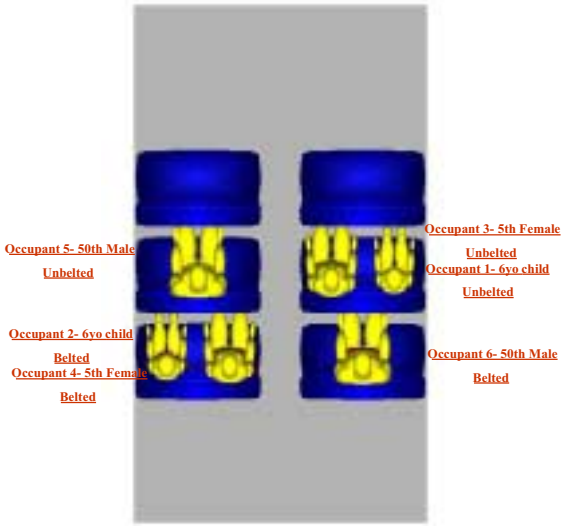

Figure 2. Occupants seating diagram for the MADYMO simulation of the sled test #3

Sled Test #6

This simulation was performed only on restrained occupants in three-point belts. The seat in this test was a prototype three-point belt system. The shoulder restraint attachment points were positioned on the outboard side of the seat for both the aisle and the window seats. The sled test included the three-point restraint with torso loading, for all available dummy sizes. The seat spacing was 19 inches.

Figure 3 illustrates the occupant seating diagram and the seat belt representation as it appears in the MADYMO model. All three occupants were modeled in MADYMO using the Hybrid III 6 year child dummy, the Hybrid III 5th percentile adult female dummy and the Hybrid III 50th percentile adult male dummy. The seat cushion of the seats located in front of the dummies were taken out, therefore they were not included in the MADYMO modeling.

The seat backs of the seats in which the dummies were positioned, were stiffened by 20% of the original stiffness in order to absorb the additional load of a shoulder restraint. The belts were constructed using membrane elements with the available finite elements in MADYMO.[4] Both the two - and three-point belts were assumed to be tightly secured to the simulated occupant.

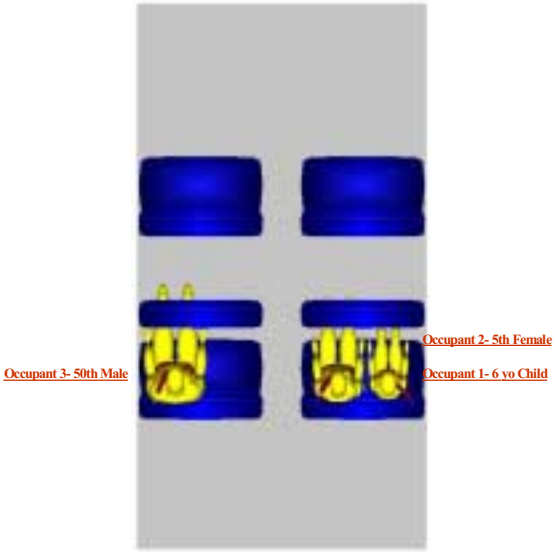

Figure 3. Occupants seating diagram for the MADYMO simulation of the sled test #6

RESULTS AND DISCUSSIONS

Frontal Rigid Barrier Test

In general, during the first half of the crash the simulated occupants of the bus first went forward in their seats, then slid slightly towards the left side of the bus and then contacted the seat in front of them with their legs, chest and head. In the second part of

the crash, the occupants started to slide back towards the rear of the bus.

Simulation and test results are compared for both the head resultant and chest resultant accelerations. The signals are compared based on six evaluation criteria designed by M. H. Ray.[5] The evaluation criteria were derived to compare MADYMO results to actual test results. Various correlation factors are evaluated using "acceptability criteria" based on vehicle crash simulation work done at NHTSA, Federal Highway Administration (FHWA), George Washington University (GWU) and others. The derived acceptable tolerance levels are as follows:

- the average residual is less than 5% of the peak value for reference signal;
- the standard deviation is less than 20% of the peak value for the reference signal;
- the percentage within the 4G corridor is when 90% of the signal reside within a corridor of ± 4G's around the reference signal;
- the correlation factor is greater than 0.80;
- the T statistic is less than 2.58; and
- the 0 (zero) Moment difference is less than 20%.

Table 1 indicates the values obtained with various evaluation criteria. The acceptable comparison criteria are displayed with a gray background. Tables 2, 3 and 4 indicate the HIC, neck injuries, chest acceleration and femur loads of the three simulated occupants from the test and simulation. The maximum values of the neck injuries are obtained in the compression-flexion mode (CF) as indicated in Table 2. The Injury Assessment Reference Value (IARV)[6] is indicated in the same tables.

Table 1. Evaluation criteria - acceptable and unacceptable values for the head and chest resultant accelerations of simulated occupants #1, 3 and 4

OCC	Avg Res %	Std Dev of Res %	% > 4G	Cor Facto	T St	0 Mom
1. 50th M Head R.	0.53	15.43	52.87	0.834	2.09	0.034
1. 50th M Chest R.	0.73	25.07	34.92	0.81	1.78	0.027
3. 6 yo Head R.	1.03	17.31	42.2	0.786	3.66	0.075
3. 6 yo Chest R.	6.4	31.63	42.22	0.84	12.4	0.229
4. 5th F. Head R.	8.67	29.82	49.03	0.643	17.8	0.337
4. 5th F. Chest R.	4.04	45.46	60.95	0.462	5.44	0.133

Table 2. Head and neck injury values of the simulated occupants

OCC	HIC Tes	HIC Simulatio	Nij Test	Nij Simulatio
	IARV=700		IARV=1.0	
1- 50th	244	797	N/A	0.2007 - CF
3- 6 yo	251	1734	1.067 - C	1.7062 - CF
4- 5th	104	423	1.147 - C	1.924 - CF

Table 3. Chest acceleration and chest deflection values of the simulated occupants

OCC	Chest Clip Test (G's)	Chest Clip Simulation (G's)	Chest Def Test (mm)	Chest Defl Simulation (mm)
	IARV=60 G's		IARV = 63 mm	
1- 50th	N/A	76.2	11	39
3- 6yo	33	35.4	14	11
4- 5th	22.8	38.6	6	3

Table 4. Femur load values of the simulated occupants

OCC	L. Femur Force (N) Test	L. Femur Force (N) Simulation	R Femur Force (N) Test	R Femur Force (N) Simulation
	IARV = 10, 000 N			
1- 50th	2704	2278	2708	551
3- 6yo	1150	2303	1855	2558
4- 5th	2996	3798	2769	2150

Figure 4 shows an overlay of the head resultant acceleration-time history and the 90th Percentile upper and lower bounds for the occupant 1, the Hybrid III 50th percentile male dummy. The overall shape of the curve matches well with the criterion. Though the simulated curve falls within the ± 4G corridor 47.13% of the time (criterion: ≥90%) the confidence corridor is exceeded for a short period of time around the peak area.

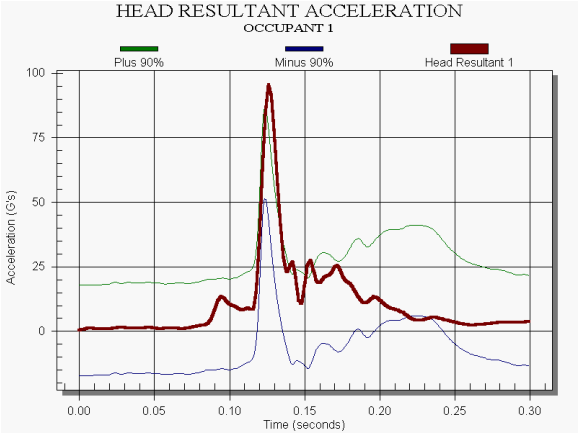

Figure 4. MADYMO Simulation head resultant acceleration of occupant 1 and the 90th percentile confidence corridor

Figure 5 details the chest resultant acceleration time-history and the 90th percentile confidence corridor. The overall shape of the curve matches well with the criterion. The correlation factor is 0.81. Even though the timing of the acceleration peaks do not match well, the curve falls well within the confidence corridor. The simulated curve falls within the ± 4G corridor 65.08 % of the time.

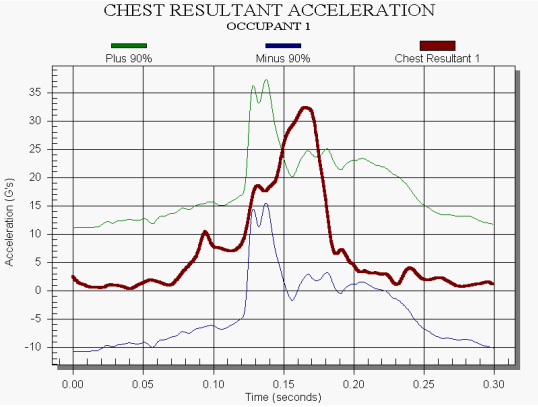

Figure 5. MADYMO Simulation chest resultant acceleration of occupant 1 and the 90th percentile confidence corridor

Figure 6 shows the head resultant acceleration signal for occupant 3, the Hybrid III 6 year old child dummy, together with the ± 4G corridor.

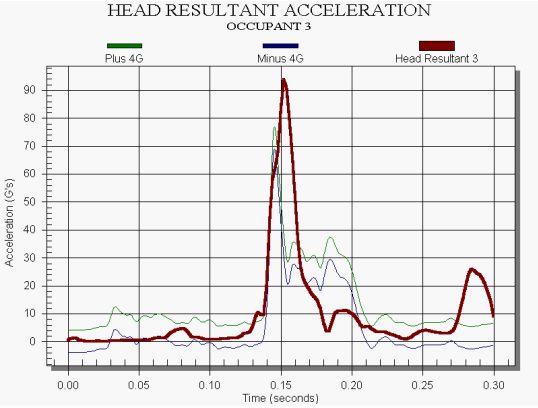

Figure 6. MADYMO Simulation head resultant acceleration of occupant 3 and the ± 4G corridor

Figure 7 shows the head acceleration signal with the 90th percentile confidence corridor. The overall shape of the simulated curve matches only part of the time (correlation factor is 0.786). There is good correlation in the shape of the signals, the simulated signal and the reference signal up to the time the peak acceleration occurs. The simulated curve falls within the ± 4G corridor 57.8% of the time. As shown in Figure 7, the simulated curve falls within the confidence corridor for most of duration.

Figure 8 details the chest resultant acceleration response for the same occupant 3. The timing of the peak occurrence matches the reference, but the simulated curve's peak magnitude is almost double the value of that of the reference signal. The overall shape of the simulated signal matches the reference signal well (the correlation factor is 0.84). The simulated curve falls with the ± 4G corridor 57.78% of the time. The simulated chest acceleration time-history curve falls within the confidence corridor relatively well.

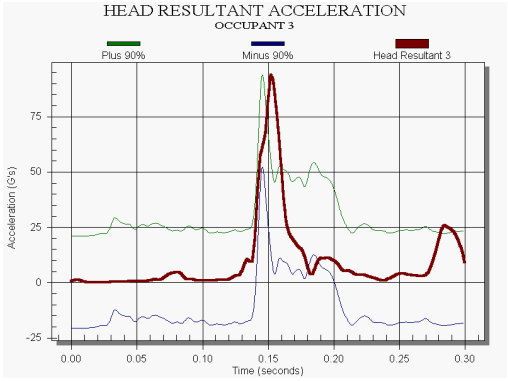

Figure 7. MADYMO Simulation head resultant acceleration of occupant 3 and the 90th percentile confidence corridor

Figure 9 shows the simulated head resultant acceleration time-history together within the ± 4G corridor. The simulated curve did not meet any of the evaluation criteria standards. The simulated curve fell with the ± 4G corridor 50.97% of the time.

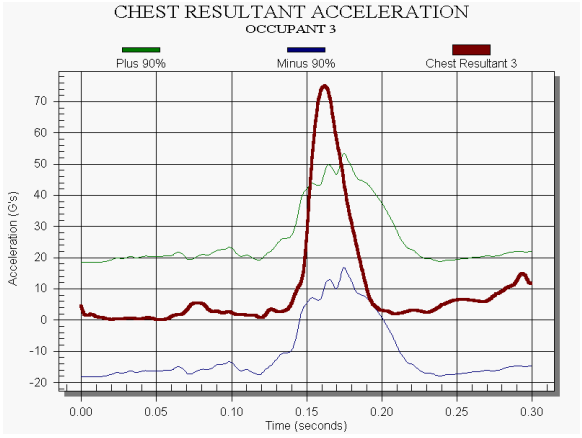

Figure 8. MADYMO Simulation chest resultant acceleration of occupant 3 and the 90th percentile confidence corridor

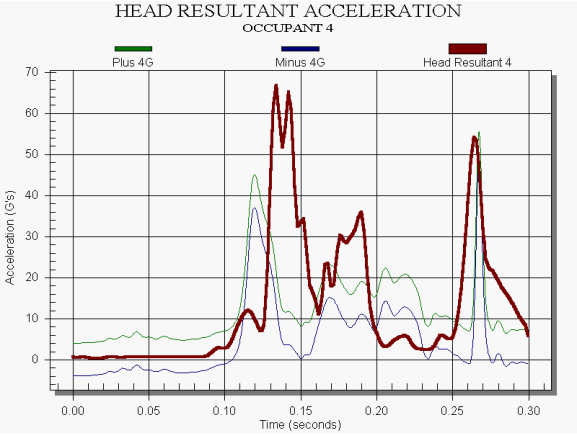

Figure 9. MADYMO Simulation head resultant acceleration of occupant 4 and the ± 4G corridor

Figure 10 indicates the upper and lower bounds of the simulated curve. The overall shapes of the reference and simulated signals match poorly. The correlation factor is only 0.643, see Table 1.

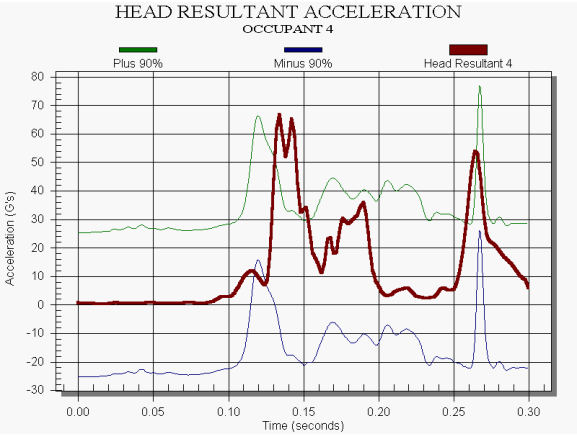

Figure 10. MADYMO Simulation head resultant acceleration of occupant 4 and the 90th percentile confidence corridor

Summary of Results

Overall, the MADYMO injury assessment values are higher for all three occupants than the values obtained in the actual test. The MADYMO simulated head and chest responses capture the main shapes of the reference signals, generally. The peak magnitudes of the simulated curves are generally higher than those of the reference curves.

Occupant 1's simulated response, kinematics and injury values are the closest to the actual test results and values. Additional research is in progress for occupants 3 and 4 to improve the simulations. The overall results of occupants 3 and 4 match, in part, the actual test's results. More consistent computer simulation results are needed for occupants 3 and 4.

Sled Test #3

The unbelted occupants first moved forward in their seats, then contacted the seat in front of them with their legs, chest and head. The impact of occupant 5 with the seat in front is very severe, causing a large plastic deformation of the seat in front. The large plastic deformation of the seats were modeled in MADYMO using a revolute joint between the seat pan and the seat back. The stiffness of the seat was defined as a torque-angle function. For the two -point restraint occupants, the pelvis was essentially fixed to the seat, after a very small translation towards the seat in front. This position resulted in a pivoting motion of the upper torso towards the seat in front.

In order to validate the simulation results, a comparison study similar to that presented in the full frontal rigid barrier test is performed. The same evaluation criteria designed by M.H. Ray[7] is used. Table 5 indicates the values obtained with various evaluation criteria. Acceptable comparison criteria are displayed with a gray background.

Table 5. Evaluation criteria - acceptable and unacceptable values for the head and chest resultant accelerations of simulated occupants #1 - 6

OCC	Avg Res.%	Std Dev of Res.%	% > 4G	Cor Factor	T St.	0 Mom
1. 6 yo Head R.	1	12.22	35.16	0.786	5.02	0.107
1. 6 yo Chest R.	0.02	15.25	25.29	0.876	0.06	0.001
2. 5th F. Head R.	0.98	13.04	27.79	0.873	4.58	0.066
2. 5th F. Chest R.	0.21	12.67	24.81	0.878	1	0.013
3. 5th F. Head R.	0.49	15.36	48.39	0.583	1.95	0.048
3. 5th F. Chest R.	1.17	28.89	43.05	0.822	2.49	0.035
4. 5th F. Head R.	0.85	9	29.61	0.897	5.82	0.069
4. 5th F. Chest R.	0.45	16.89	28.54	0.914	1.65	0.017
5. 50th M. Head R.	6.52	32.56	47.16	0.607	12.3	0.257
5. 50th M. Chest R.	1.86	15.58	31.02	0.832	7.31	0.094
6. 50th M. Head R.	0.07	15.23	54.07	0.811	0.29	0.005
6. 50th M. Chest R.	0.01	12.14	18.3	0.937	0.06	0.001

Tables 6, 7 and 8 indicate the HIC, neck injuries, chest acceleration and femur loads from the test and simulation. The IARVs[8] are indicated for all calculated injuries. The neck injury modes for which the maximum injury occurs are indicated in Table 7, where FC represents flexion-compression, ET extension-tension, FT flexion-tension and CE compression-extension.

Table 6. Head and chest injury values of the simulated occupants

OCC	HIC Test	HIC Simulation	Chest Clip Test	Chest Clip Simulation
	IARV = 700		IARV = 60 G's	
1- 6 yo C	369	87	30.6	51.0
2- 6 yo C	229	313	48.7	29.8
3- 5th F	484	304	23.5	35.0
4- 5th F	335	259	28.9	39.4
5- 50th M	269	625	39.6	30.0
6- 50th M	334	143	34.4	27.0

Table 7. Neck injury values of the simulated occupants

OCC	Nij Test	Nij Simulation
	IARV = 1.0	
1- 6 yo C	1.243 - FC	1.2553 - FC
2- 6 yo C	1.403 - ET	1.0343 - CE
3- 5th F	0.879 - FT	1.0467 - FC
4- 5th F	0.756 - FT	0.6445 - ET
5- 50th M	0.483 - ET	0.8605 - ET
6- 50th M	0.673 - ET	0.477 - ET

Table 8. Femur load values of the simulated occupants*

OCC	L Femur Test (N)	L Femur Simulation (N)	R Femur Test (N)	R Femur Simulation (N)
	IARV = 10, 000 N			
1- 6 yo C	3576	834	1810	871
2- 6 yo C	423	258	378	266
3- 5th F	906	3950	461	3983
4- 5th F	1209	1668	1308	1628
5- 50th M	***	937	***	1508
6- 50th M	2470	548	1989	731

Figure 11 shows an overlay of the head resultant acceleration time-history and the 90th percentile confidence corridor for unbelted occupant 1, the Hybrid III 6 year old child dummy. The simulated curve falls well within the 90th percentile confidence corridor. Though the timing of the peak occurrence is very good, its magnitude is higher in the simulated curve. The overall shape of the simulated curve matches the reference signal most of the time. The simulated curve falls within the ± 4G corridor 64.87% of the time.

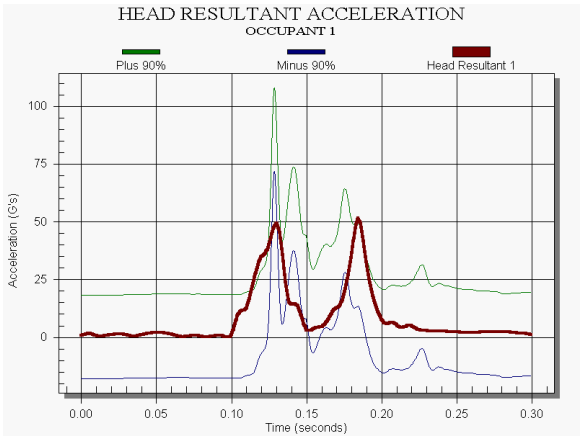

Figure 11. MADYMO Simulation head resultant Acceleration of Occupant 1 and the 90th percentile confidence corridor

Figure 12 details the chest resultant acceleration for occupant 1 together with the confidence interval. The simulated curve follows the shape of the reference signal very well until the occurrence of the second peak. The overall shape of the signals match well as indicated by the value of 0.876 of the correlation factor. The simulated curve falls within the ± 4G corridor 74.71% of the time. Three out of six evaluation criteria are acceptable values, see Table 5.

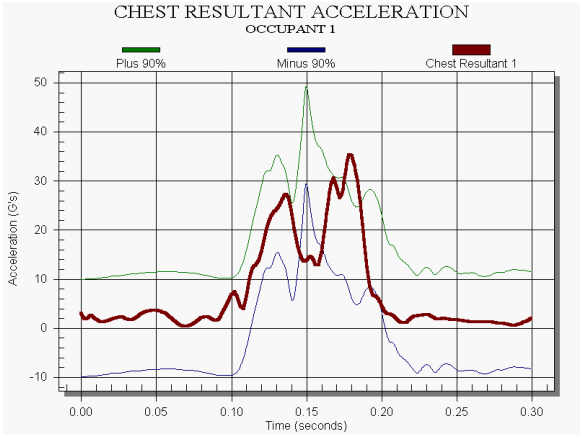

Figure 12. MADYMO Simulation chest resultant acceleration of occupant 1 and the 90th percentile confidence corridor

Figure 13 shows the head resultant acceleration time-history for belted occupant 2, the Hybrid III 6 year

*Due to the separation of the seat cushion from the seat structure in the full-scale test, the MADYMO representation of occupant 5 was not considered.

old child dummy and the ± 4G corridor. Figure 14 details the head resultant acceleration and confidence corridor for occupant 2. The timing of the peak occurrences and the overall shape of the simulated signal with the reference signal match very well, as shown in Figure 13. The simulated curve falls within the ± 4 G corridor 72.21% of the time. Four out of six evaluation criteria values are acceptable, see Table 5.

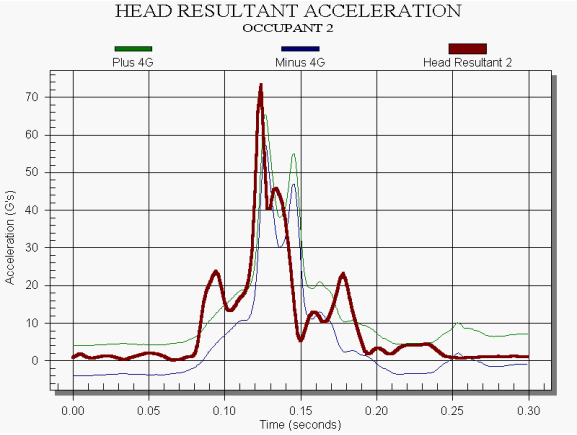

Figure 13. MADYMO Simulation head resultant acceleration of occupant 2 and the ± 4G corridor

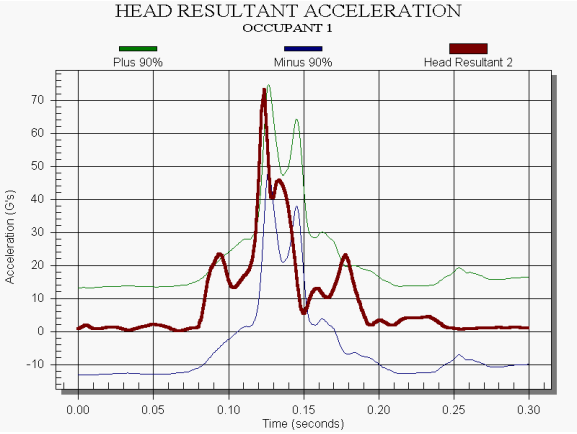

Figure 14. MADYMO Simulation head resultant acceleration of occupant 2 and the 90th percentile confidence corridor.

The chest resultant acceleration time-history of occupant 2 is presented in Figure 15 together with the upper and lower confidence limits. Four out of six evaluation criteria are acceptable, as indicated in Table 4. The simulated curve falls within the ± 4G corridor 75.19% of the time. The timing of the peak acceleration of the simulated curve matches with that of the reference signal very well. The overall shape of the simulated curve matches the reference curve well.

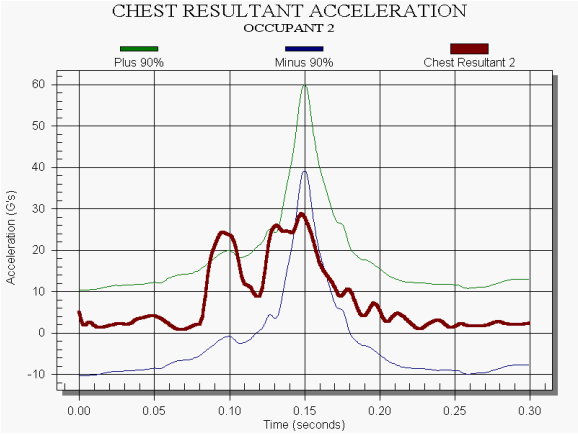

Figure 15. MADYMO Simulation Chest Resultant Acceleration of occupant 2 and 90th percentile Confidence corridor.

Occupant 3's head resultant acceleration time-history is represented in Figure 16 together with the confidence corridor. As indicated in Table 5, four out of six evaluation criteria are met for the head response of the unbelted Hybrid III 5th percentile adult female dummy. The simulated curve falls within the ± 4G corridor 51.61% of the time.

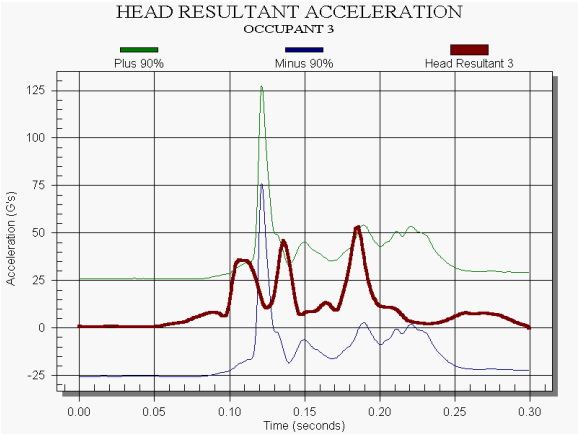

Figure 16. MADYMO Simulation Head resultant acceleration of occupant 3 and the 90th percentile confidence corridor

The overall shape of the simulated curve matches poorly the reference curve with a correlation factor of only 0.583. Even though the simulated curve falls within the confidence limits, it fails to capture the peak of the reference acceleration.

Figure 17 shows the chest resultant acceleration of occupant 3 and the 90th Percentile confidence limits. The overall shape matches well with a correlation factor of 0.822. Even though the timing of the acceleration peaks does not match well, the simulated curve falls well within the confidence margins. The

simulated curve falls within the ± 4G corridor 56.95% of the time.

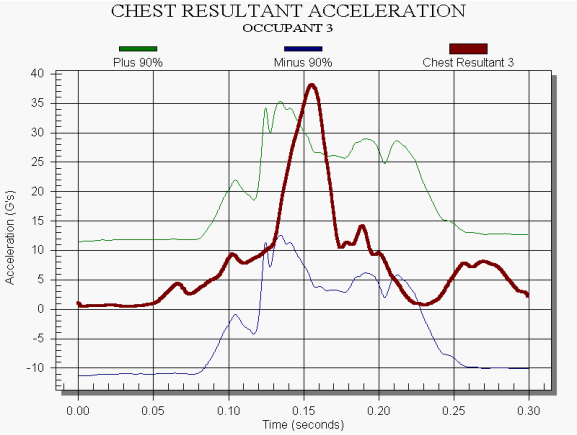

Figure 17. MADYMO Simulation Chest Resultant acceleration of Occupant 3 and 90th Percentile confidence corridor

For the belted occupant 4 the head resultant acceleration time-history and the ± 4G limits are shown in Figure 18. The simulated curve captures the shape of the reference signal very well as shown in Figure 18. The timing of the peak acceleration is very well matched by the simulated signal. The simulated curve falls within ± 4G corridor 70.40% of the time and it is well within the confidence limits as shown in Figure 19.

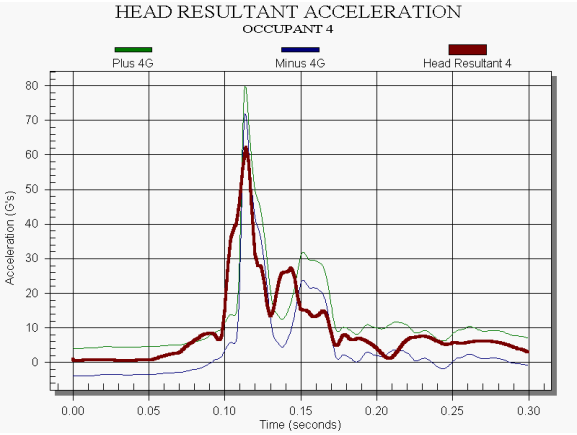

Figure 18. MADYMO Simulation head resultant acceleration of occupant 4 and ± 4G corridor

Figure 20 details the chest resultant acceleration of occupant 4. The general shape of the simulated curve matches the reference signal well with a correlation factor of 0.914, see Table 5. The timing of the peak acceleration of the simulated curve does not match the reference curve. As shown in Figure 20 there is a small delay of 20 milliseconds in the simulated response. The simulated curve falls well within the confidence limit. Two out of six criteria elements are satisfied.

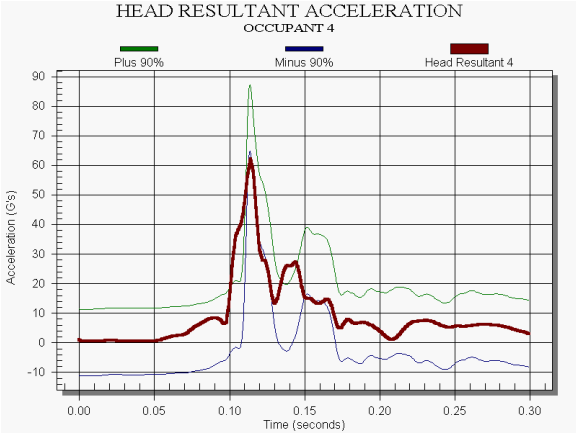

Figure 19. MADYMO Simulation head resultant acceleration of occupant 4 and the 90th percentile confidence corridor

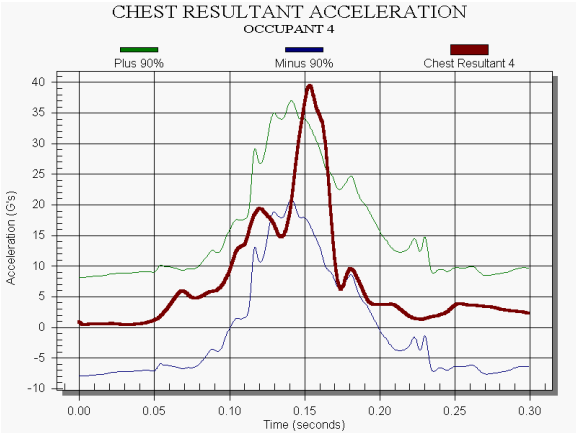

Figure 20. MADYMO Simulation chest resultant acceleration of occupant 4 and the 90th percentile confidence corridor

In the first half of the simulation there was a severe impact of occupant 5, the unbelted Hybrid III 50th percentile adult male dummy, with the seat in front. In the sled test performed by NHTSA, the seat cushion in front of occupant 5 separated from the seat structure due to the severity of the impact. For consistency purposes no separation of the seats was modeled in MADYMO, therefore the seat in front of occupant 5 deformed plastically, but did not fail when impacted by occupant 5. Not modeling the separation of the seat in MADYMO affected, to some extend, the overall kinematics of occupant 5.

Figures 21 and 22 show the simulated response of the head and chest of occupant 5. The overall shape of the simulated chest response matches the test signal well, with a correlation factor of 0.832, but the

timing of the peak acceleration of the simulated curve is shifted to the left compared to the reference curve. The simulated chest response captures the reference chest signal much better, with four out of six criteria elements satisfied compared to the simulated head response that does not meet any of the criteria elements.

Figure 23 shows the simulated head resultant acceleration time-history of belted occupant 6, the Hybrid III 50th percentile adult male dummy. The simulated head response and the reference signal correlate very well, with five out of six criteria elements satisfied. The shape of the simulated curve matches the test signal, with a correlation factor of 0.811, see Table 5. There is a slight time lag in the simulated head response most likely attributed to the loading of the two-point belt. The MADYMO head resultant curve falls within the ± 4G corridor 46 % of the time. The simulated curve falls well within the confidence corridor.

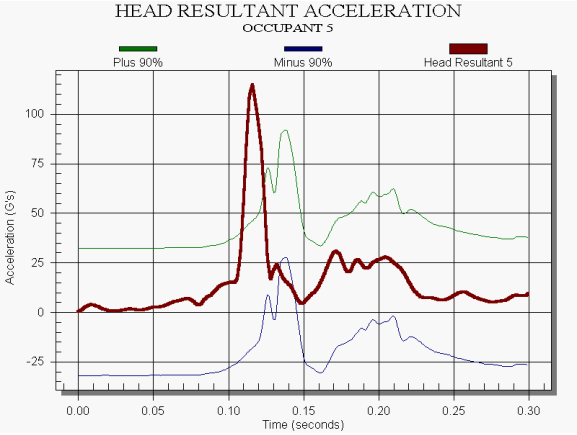

Figure 21. MADYMO Simulated head resultant acceleration of occupant 5 and the 90th percentile confidence corridor

The simulated chest response is presented in Figure 24, indicating a good match with the test response. The general shape of the simulated curve matches the reference signal, with a correlation factor of 0.937, see Table 5. The timing of the peak acceleration is delayed slightly in the MADYMO simulation. The simulated chest response falls within the ± 4G 81.7% of the time. Five of the six criteria elements are satisfied.

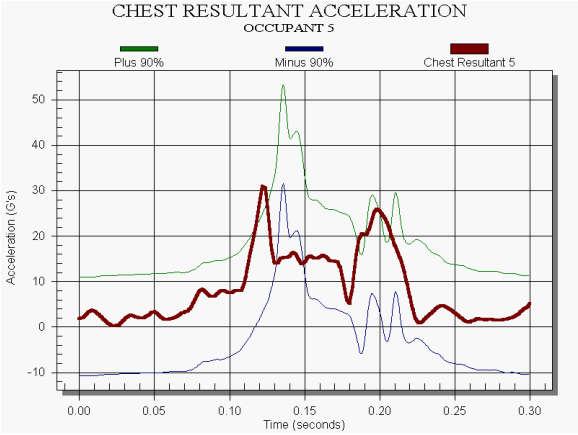

Figure 22. MADYMO chest resultant acceleration of occupant 5 and the 90th percentile confidence corridor

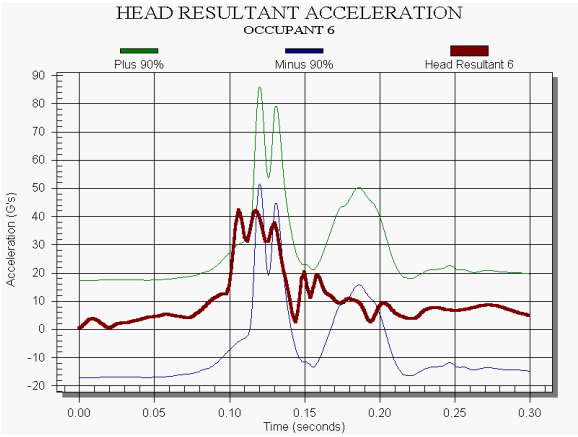

Figure 23. MADYMO Head resultant acceleration of occupant 6 and 90th percentile confidence corridor

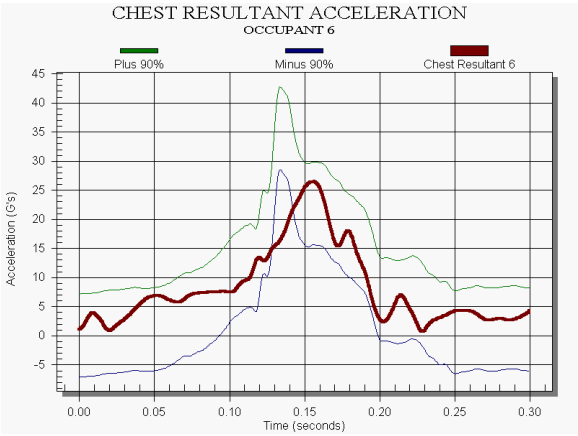

Figure 24. MADYMO Simulated chest resultant acceleration of occupant 6 and 90th percentile confidence corridor

Summary of Results

MADYMO's overall results for occupants 2, 3, 4 and 6 are good. The computer simulation program captures the overall occupant kinematics well. The injury assessment values are comparable to those obtained in the actual test and the head and chest simulated responses correlate with the reference curves. Occupant 1's MADYMO response is generally good, but more work in the computer modeling could improve the results.

Due to the separation of the seat cushion from the seat structure in the full-scale test, the MADYMO representation of occupant 5 was not considered for this validation.

Sled Test #6

The three-point belted simulated occupants demonstrated similar kinematics as the two-point belted occupants in sled test #3, but with less movement of the upper body. The torso belt limits the forward movement of the occupants, therefore the impact with the seat in front was not as severe as in the two-point restrained case. For the first half of the simulation all occupants moved forward, but only occupants 2 and 3 contacted the seat in front with their heads. There was no upper body contact of occupant 1 with the seat in front. After the first half of the simulation the torso belt pulled the occupants backward towards their original seating position.

For validating the results, a similar comparison study as in the previous two cases analyzed before, was performed. Based on the M.H. Ray[9] evaluation criteria method various correlation factors are calculated and output, see Table 9. Tables 10, 11 and 12 indicate the head, chest and neck injuries as well as the femur loads for the simulated occupant. The neck injury modes for which the maximum injury occurs are indicated in Table 11, where FT represents flexion-tension, ET extension-tension, CE compression-extension and CF compression-flexion.

Table 9. Evaluation criteria - acceptable and unacceptable values for the head and chest resultant accelerations of the simulated occupants

OCC	Avg Res.%	Std Dev of Res %	% > 4G	Cor Facto	T St	0 Mom
1. 6 yo Head R.	3.93	11.95	27.54	0.961	18.4	0.148
1. 6 yo Chest R.	4.93	14.12	21.61	0.939	21.4	0.142
2. 5th F. Head R.	1.55	24.33	48.95	0.785	3.89	0.06
2. 5th F. Chest R.	2.42	15.9	23.79	0.942	9.31	0.073
3. 50th M Head R.	0.07	9.73	28.49	0.855	0.42	0.007
3. 50th M. Chest R.	0.04	15.82	24.54	0.956	0.14	0.001

Table 10. Head and chest injury values of the simulated occupants

OCC	HIC Test	HIC Simulation	Chest Clip Test (G's)	Chest Clip Simulation (G's)
	IARV = 700		IARV = 60 G's	
1- 6 yo C	88	208	23.10	24.6
2- 5th F	56	188	21.30	22.7
3- 50th M	419	49	19.80	16.5

Table 11. Neck injury values of the simulated occupants

OCC	Nij Test	Nij Simulation
	IARV = 1.0	
1- 6 yo C	0.460 - FT	0.5624 - CE
2- 5th F	0.330 - ET	0.5249 - CE
3- 50th M	0.363 - ET	0.1356 - CF

Table 12. Femur load values of the simulated occupant

OCC	L Femur Test (N)	L Femur Simulation	R Femur Test (N)	R Femur Simulation
	IARV = 10, 000 N			
1- 6 yo C	289	289	291	315
2- 5th F	256	887	277	881
3- 50th M	4398	855	2099	1160

Figure 25 details the simulated head resultant acceleration of occupant 1, the Hybrid III 6 year old child dummy. The simulated curve falls well within the confidence limits. The overall shape of the reference signal and simulated signal match well with a correlation factor of 0.961. The simulated response falls within the ± 4G corridor 72.5% of the time. The head response does not capture the magnitude of the peak in the reference signal very well, but overall, the simulated signal has four out of six criteria elements satisfied, see Table 9.

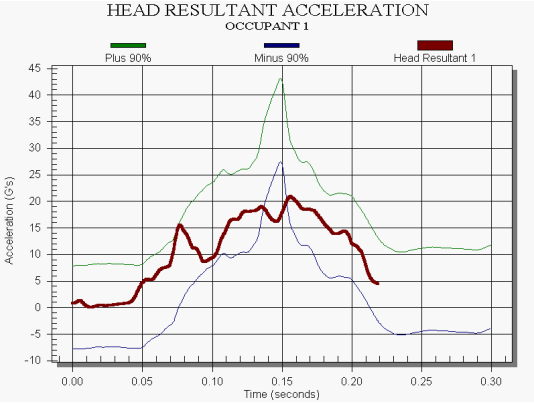

Figure 25. MADYMO Simulated head resultant acceleration of occupant 1 and the 90th percentile confidence corridor

The chest response for occupant 1 is presented in Figure 26. The simulated curve falls almost perfectly within the confidence boundaries. With a correlation factor of 0.939, see Table 8, the simulated response follows the reference signal relative closely. The chest response falls within the ± 4G corridor 78.4% of the time. Four out of six evaluation criteria are met, see Table 9.

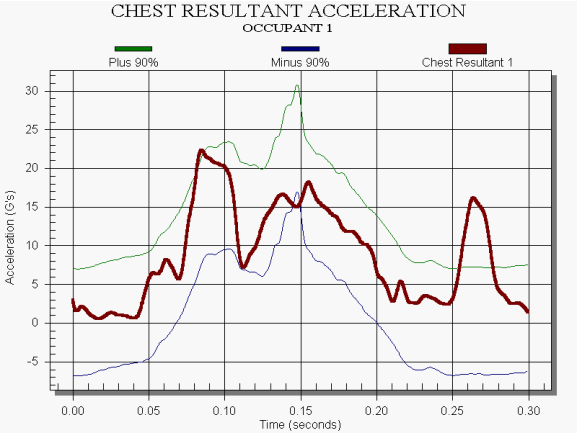

Figure 26. MADYMO Simulation chest resultant acceleration of occupant 1 and the 90th percentile confidence corridor

Figure 27 shows the head resultant acceleration for occupant 2, the Hybrid III 5th percentile adult female dummy, and as shown in Figure 27 there is a poor correlation between the two signals (correlation factor is 0.785, see Table 9). Two spikes appear earlier in the simulated curve, but not in the reference signal. This indicates that the occupant 2 impacted the seat in front earlier and harder than in the physical test. The curve falls well within the confidence limits, and it stays within the ± 4G corridor 51% of the time. As shown in Table 9, only two out of six evaluation factors are satisfied.

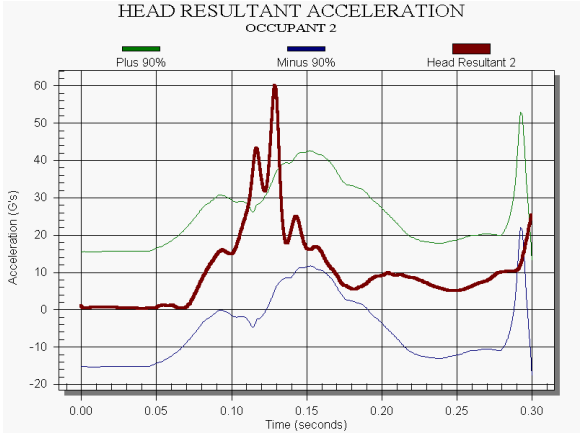

Figure 27. MADYMO Simulation head resultant acceleration of occupant 2 and the 90th percentile confidence corridor

The simulated chest response for the occupant 2 and the confidence boundaries are presented in Figure 28. The overall shape of the simulated signal matches the reference curve with a correlation factor of 0.942. There is a slightly earlier occurrence of the peak in the simulated curve, but the general shape of the reference signal is captured well. The simulated chest response falls within the ± 4G corridor 84.10% of the time. Four out of six criterial elements are satisfied, see Table 9.

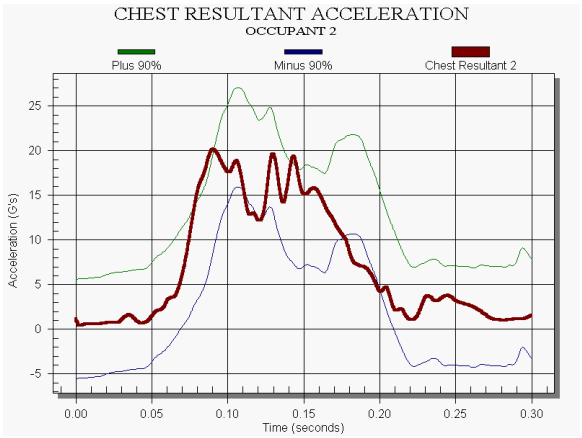

Figure 28. MADYMO Simulation chest resultant acceleration of occupant 2 and the 90th percentile confidence corridor

The simulated head and chest responses for occupant 3, the Hybrid III 50th Percentile adult male dummy, are shown in Figure 29 and 30, respectively.

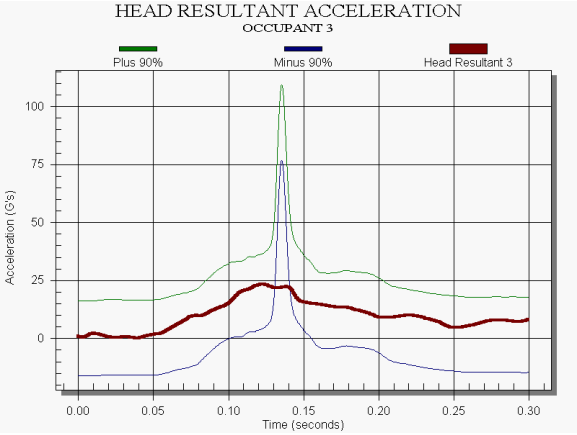

Figure 29. MADYMO Simulation head resultant acceleration of occupant 3 and the 90th percentile confidence corridor

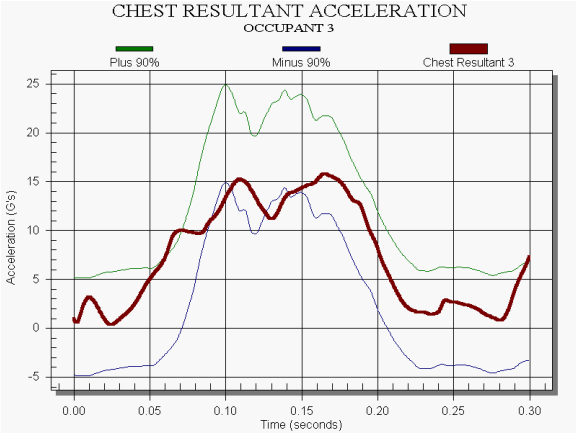

Figure 30. MADYMO Simulation chest resultant acceleration of occupant 3 and the 90th percentile confidence corridor

Though the peak acceleration is not showing in the simulated curve, the main shape of the reference curve is captured well. The head resultant values show good agreement in timing, but not in magnitude. The higher value of the peak in the reference acceleration curve, compared to the MADYMO simulated curve, is due to a more severe head impact of occupant 3 to the seat in front This is most likely because the torso belt in the physical test allows the occupant to move forward more than the torso belt in the MADYMO simulation. The overall shape of the simulated curve matches the reference signal with a correlation factor of 0.855. The simulated curve falls within the ± 4G corridor 71.5% of the time. The MADYMO simulated head response is in good accordance with the reference signal. Five out of six criteria elements are satisfied, see Table 9.

As shown in Figure 30 there is a very good correlation between the simulated curve and the reference curve. The curve falls almost perfectly within the confidence boundaries, and it captures well the overall shape of the reference signal (correlation factor is 0.956, see Table 9). The simulated chest response falls within the ± 4G corridor 75.46% of the time. Five out of six evaluation criteria are met.

Summary of Results

MADYMO's overall results for occupants 1 and 3 are reasonably good. With the exception of the head injury assessment value for occupant 3, the simulated injury assessment values matched those of the actual test relatively well. Occupant 2's MADYMO response, overall kinematics and injury assessment values are fairly good compared to the actual test. However more modeling work is necessary to improve the occupant's head response.

CONCLUSIONS

The MADYMO software package proved to be a tool that could be used in studying the kinematics and injury assessments for the selected tests, and therefore it can be used in future studies that focus on occupant protection systems evaluation.

In order to evaluate the performance of each restraint strategy, the sled tests performed simulating the frontal crash mode included compartmentalization, lap-only belts, and lap/shoulder belts. Three loading conditions were simulated: (1) belted occupants without any loading from occupants seated behind them, (2) belted occupants with loading from unbelted occupants seated behind them, and (3) unbelted occupants into the seat back in front of them.

In terms of compartmentalization, ATDs performed well overall, although some neck injury values exceeded injury limits. Compartmentalization worked best for smaller occupants. The larger rear seated occupants tend to override the standard height seat back. With regards to the lap belt protection

system, ATDs restrained by lap belts only had slightly higher neck injury values than in compartmentalization testing (the neck injury values may be sensitive to seat spacing in this case). However, the lap belt system prevents the larger rear, unbelted ATD's from overriding the seat back.** ATDs performed best overall when properly restrained in lap/shoulder belt systems. Adjustable shoulder belts were not available on either system. An adjustable shoulder belt device would have provided a better belt fit for the 6 year old and 5th percentile adult female. The lap/shoulder belt system prevented the larger ATDs from overriding the seat back. However, the resulting stiffer seat backs may cause higher injury values for the unrestrained or improperly restrained occupants.

The MADYMO computer simulation software has several limitations, including a number of assumptions necessary to simulate the vehicle and occupant dynamics and a more simplistic manner of defining the occupant to occupant contacts, or occupant to vehicle interior contacts. Therefore, it is important that consideration of these limitations be taken into account in drawing conclusions based on these simulations. Nonetheless, the main focus of this work is to find a reasonable and reliable base for comparing various restraint conditions – compartmentalization, lap belt, lap/shoulder belt, or variations these restraint systems. One potential method to efficiently and accurately simulate real world crash tests using MADYMO would be to introduce a finite element seat model. This type of seat representation would allow a more accurate definition of the contact deformation functions between the occupant and the seats.

FUTURE RESEARCH

Future work will focus on using real world testing and computer simulations to evaluate various crash scenarios and test conditions that would help in evaluating occupant protection systems. As it has already been shown by a series of sled tests conducted by NHTSA, a balance among the seat characteristics (seat back height, padding, stiffness, etc.), the restraint type and occupant sizes is needed.

REFERENCES

1. MADYMO, User's Manual 3D Version 5.4, May 1999, Copyright 1999, TNO Automotive.

2. *Ibid.*

3. *Ibid.*

4. *Ibid.*

5. M. H. Ray, "Repeatability of Full-Scale Crash Tests and Criteria for Validating Finite Element Simulations", Transportation Research Record No. 1528, Transportation Research Board, Washington, DC, 1996.

6. 49CFR.571.208, "Occupant Crash Protection".

7. Ray, "Repeatability of Full-Scale Crash Tests and Criteria for Validating Finite Element Simulations", 1996.

8. 49CFR.571.208, "Occupant Crash Protection".

9. Ray, "Repeatability of Full-Scale Crash Tests and Criteria for Validating Finite Element Simulations", 1996.

**It should be noted that the Hybrid III dummies may have some limitations in identifying abdominal and spinal injuries. There is concern regarding the biofidelic capability of the Hybrid III pelvis.